

## Zinc Porphyrin-Cored Dendrimers; Axial Coordination of Pyridine and Photoinduced Electron Transfer to Methyl Viologen

Ji Eun Park, Daeock Choi, and Eun Ju Shin\*

Department of Chemistry, Suncheon National University, Suncheon, Jeonnam 540-742, Korea. \*E-mail: ejs@sunchon.ac.kr  
Received September 2, 2011, Accepted October 6, 2011

The porphyrin-incorporated aryether dendrimers ZnP-D1 and ZnP-D4 were investigated to discover the influence of dendritic environments for the axial ligation of pyridine and photoinduced electron transfer by methyl viologen. Absorption and fluorescence spectra of ZnP, ZnP-D1, and ZnP-D4 were measured in dichloromethane with the addition of pyridine or methyl viologen dichloride. Axial ligation of pyridine was confirmed by red-shifted absorption spectrum. The complex formation constants  $K_f$  (Table 1) for axial coordination of pyridine on ZnP, ZnP-D1, and ZnP-D4 were estimated to be  $4.4 \times 10^3 \text{ M}^{-1}$ ,  $3.3 \times 10^3 \text{ M}^{-1}$ , and  $1.7 \times 10^3 \text{ M}^{-1}$ , respectively. The photoinduced electron transfer to methyl viologen dichloride was confirmed by fluorescence quenching. Stern-Volmer constants  $K_{sv}$  for ZnP, ZnP-D1, and ZnP-D4 were calculated to be  $2.6 \times 10^3$ ,  $2.5 \times 10^3$ , and  $2.1 \times 10^3$ , respectively. ZnP-D4 surrounded by 4 aryl ether dendrons shows the smallest  $K_f$  and  $K_{sv}$  values, with comparison to ZnP and ZnP-D1.

**Key Words :** Arylether dendrimer, Zinc porphyrin, Axial coordination, Pyridine, Methyl viologen

### Introduction

In Nature, light energy is converted into chemical energy by natural photosynthesis. Mimicry of natural photosynthesis leads to design and development of a variety of artificial photosynthetic systems such as solar cells.<sup>1-12</sup> Metalloporphyrin is a key compound for light energy harvesting and long-range electron transfer to reaction center in plants and photosynthetic bacteria. Porphyrin is not only a well-known luminescent and redox active compound that can accomplish the photoinduced electron transfer in photosynthetic reaction center, but also is frequently observed in porphyrin-containing enzyme manifesting the enzyme activity by carrying out the axial coordination on central metal of metalloporphyrin plane. Numerous research groups have designed and prepared the molecular energy storage/photonic/electronic devices containing porphyrin moiety.<sup>1-12</sup>

Structural uniqueness of dendrimer<sup>13,14</sup> allows feasible molecular design and well-defined array, in which the position of porphyrin and other functional groups is precisely controlled. The introduction of porphyrins into dendritic structures has received great attention since the early days of dendrimer chemistry as mimicry of natural hemoproteins or natural photosynthetic systems.

Porphyrin dendrimers<sup>15,16</sup> have features of both desirable photophysical and redox properties of porphyrins and synthetically controllable structure of dendrimers. Various porphyrin dendrimers have been studied for a variety of applications to the functional molecular devices including artificial photosynthesis and optoelectronic device.<sup>17-34</sup>

This paper deals with how the dendritic environments of porphyrin-centered dendrimers affect the axial coordination of pyridine on central zinc porphyrin moiety as a model of metalloporphyrin-containing enzyme, and the photoinduced

electron transfer from central zinc porphyrin moiety to electron acceptor methyl viologen as a model of artificial photosynthetic system.

### Experimental Section

**Spectroscopic Measurements.** Absorption spectra were recorded on a Shimadzu UV-2401PC spectrophotometer. Steady-state fluorescence spectra were recorded on a SLM-Aminco AB2 luminescence spectrophotometer. The concentrations were controlled so that the absorbances of the solutions at the excitation wavelength of 550 nm have the value of 0.07-0.08, to avoid inner filter effects.

**Materials.** Syntheses of ZnP, ZnP-D1, and ZnP-D4 (See Figure 1) were previously reported.<sup>35</sup> Pyridine and methyl viologen dichloride was purchased from Aldrich Chemical Co. Methylene chloride and other solvents were purchased from DAE JUNG Chemical Co. and were dried and distilled by general purification methods.

### Results and Discussion

**Axial Coordination of Pyridine on Dendrimers with Zinc Porphyrin Core.** It is well-known that zinc porphyrin forms stable five- or six-coordinated complexes with coordinating ligands.<sup>36-38</sup> Axial coordination of a ligand on zinc porphyrin provides a feasible construction of multicomponent molecules through noncovalent self-assembly. One of strategies to construct readily dendrimers of higher order is to build noncovalent self-assembly, for example, by coordination complex formation between zinc porphyrin-tethered dendrimer and pyridine-tethered dendrimer. Therefore, we wonder how the complicated environment caused by spatial dendrimer structure affects axial coordination between zinc

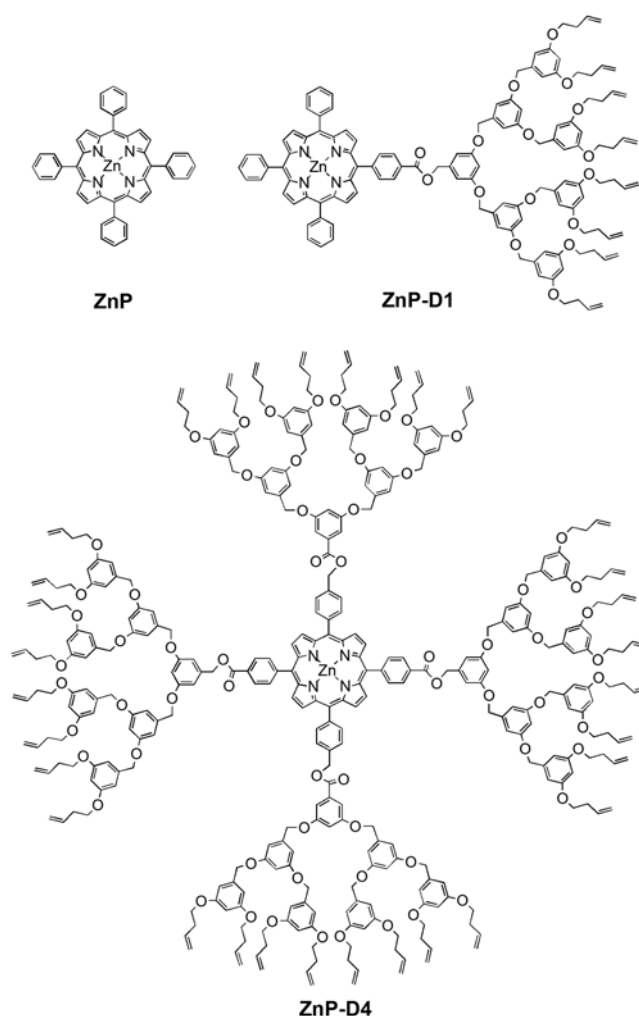


**Figure 1.** Structures of ZnP, ZnP-D1, and ZnP-D4.

porphyrin and pyridine.

As a model study, axial ligation of pyridine itself on dendrimers with zinc porphyrin core and the influence of dendritic environment were investigated by observing the absorption and fluorescence spectra of zinc porphyrin-cored dendrimers with addition of pyridine. On complexation of zinc porphyrin with an axial ligand, two effects are often seen in the UV-vis absorption spectrum: a red shift of the entire spectrum relative to zinc porphyrin itself and an increase in the  $\epsilon_{\alpha}/\epsilon_{\beta}$  ratio of the two visible bands. Thus, one could use the wavelength shift and intensity ratio of the visible bands as a measure of the degree of axial ligation.<sup>37</sup>

The structures of zinc 5, 10, 15, 20-tetraphenylporphyrin (ZnP) and zinc porphyrin-cored dendrimers used in this study (ZnP-D1, and ZnP-D4) and their complex with pyridine are shown in Figure 1 and Figure 2, respectively.

Absorption spectra are similar for ZnP, ZnP-D1, and ZnP-D4, except that absorption intensity at 280 nm increases in the higher generation of dendrimer. Fluorescence spectra are also similar with two bands for ZnP, ZnP-D1, and ZnP-D4, although fluorescence intensity ratio of shorter wavelength emission band to longer wavelength band varies with the generation of dendrimer.

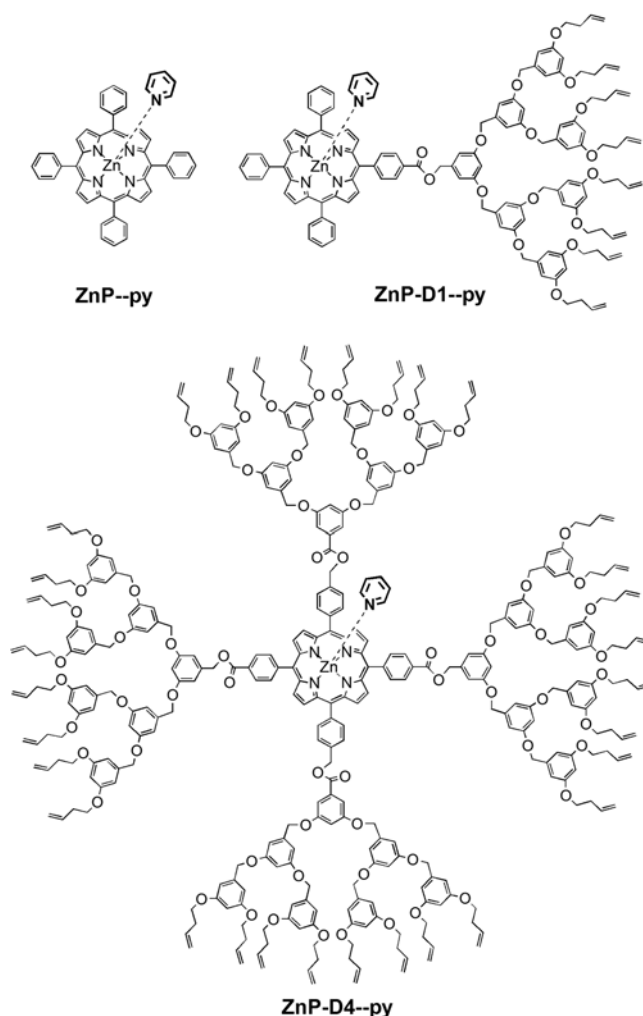


**Figure 2.** Axial coordination of pyridine on ZnP, ZnP-D1, and ZnP-D4.

As shown in Figure 3, Figure 4, and Table 1, absorption maxima, the intensity ratios  $\epsilon_{\alpha}/\epsilon_{\beta}$  of two Q bands, and fluorescence maxima of ZnP, ZnP-D1, and ZnP-D4 in dichloromethane show appreciable changes with adding pyridine, indicating axial coordination of pyridine.

Axial coordination of pyridine on ZnP, ZnP-D1, or ZnP-D4 was investigated by observing the UV-vis absorption spectra (Figure 3) of ZnP, ZnP-D1, and ZnP-D4 of  $\sim 1 \times 10^{-5}$  M in dichloromethane with addition of pyridine (0, 1, 2, 5, 10, 15, 20, 25, 30, 40, 50 equiv.). Figure 4 shows fluorescence spectra of ZnP, ZnP-D1, or ZnP-D4 of  $\sim 1 \times 10^{-5}$  M in dichloromethane with addition of pyridine (0, 1, 2, 5, 10, 15, 20, 25, 30, 40, 50 equiv.) at excitation wavelength of 558 nm. Table 1 summarized absorption maxima, fluorescence maxima for ZnP, ZnP-D1, ZnP-D4 and their coordinated complexes in dichloromethane, and the complex formation constant  $K_f$  for axial coordination of pyridine.

In the absence of pyridine, absorption spectrum of ZnP in dichloromethane shows Soret band around 418 nm and Q bands around 547 nm ( $\beta$  band) and 585 nm ( $\alpha$  band). As shown in Figure 3(a) and Table 1, upon addition of pyridine, intense Soret band and two Q bands of ZnP in dichloro-

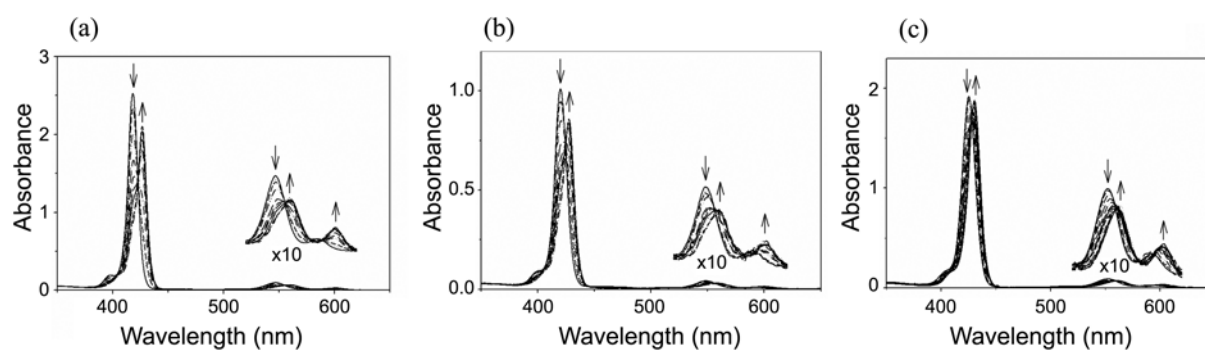


**Figure 3.** Absorption spectral change of ZnP (a), ZnP-D1 (b), and ZnP-D4 (c) of  $\sim 1 \times 10^{-5}$  M with addition of pyridine (0, 1, 2, 5, 10, 15, 20, 25, 30, 40, 50 equiv.) in dichloromethane.

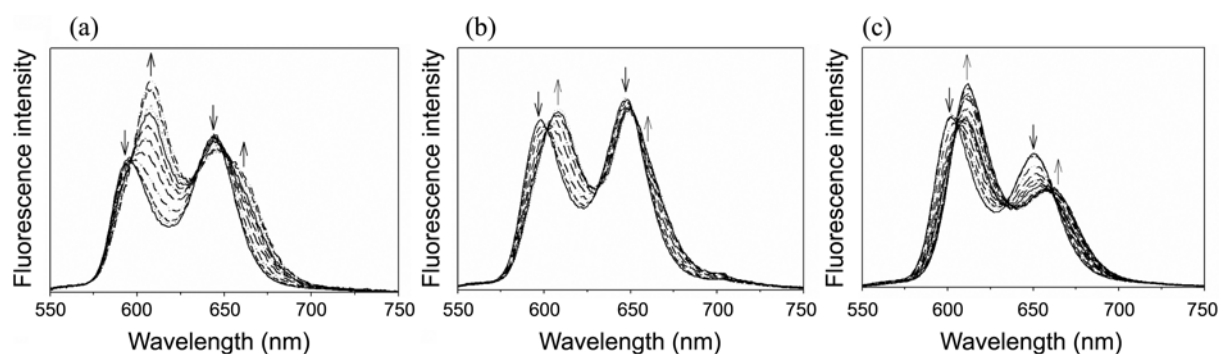


**Figure 4.** Fluorescence spectral change of ZnP (a), ZnP-D1 (b), or ZnP-D4 (c) of  $\sim 1 \times 10^{-5}$  M with addition of pyridine (0, 1, 2, 5, 10, 15, 20, 25, 30, 40, 50 equiv.) in dichloromethane.

**Table 1.** Absorption maxima ( $\lambda_a^{\max}$ ), fluorescence maxima ( $\lambda_f^{\max}$ ), and formation constant ( $K_f$ ) for ZnP, ZnP-D1, ZnP-D4 and their coordinated complexes in dichloromethane

Compound	[pyridine]/ [compound]	$\lambda_a^{\max}$ , nm				$\lambda_f^{\max}$ , nm	$K_f$ , $M^{-1}$
		Soret band	Q band				
			$\beta$	$\alpha$	$\epsilon_\alpha/\epsilon_\beta$		
ZnP	0	418	547	585	0.16	596, 644	$4.4 \times 10^3$
	50	427	561	602	0.46	608, 647	
ZnP-D1	0	420	548	590	0.23	598, 648	$3.3 \times 10^3$
	50	428	560	602	0.47	608, 651	
ZnP-D4	0	426	552	592	0.35	602, 650	$1.7 \times 10^3$
	50	431	564	603	0.53	611, 661	

methane were red-shifted to 427 (+9), 561 (+14), and 602 (+17) nm with the appearance of isosbestic points in 423 and 555 nm, indicating the formation of 1:1 complex through the axial coordination of pyridine on ZnP. The intensity ratio  $\epsilon_\alpha/\epsilon_\beta$  of two Q bands increased 2.9 fold from 0.16 to 0.46. Fluorescence maxima of ZnP were also red-shifted from 596 and 644 nm to 608 (+12) and 647 (+3) nm on axial ligation of pyridine (Figure 4(a) and Table 1). The fluorescence emission of ZnP was not only red-shifted up to 10 nm but also fluorescence intensity of short wavelength band was enhanced to *ca.* 1.6 fold with addition of pyridine. Fluorescence enhancement may be due to the increased electron density of core zinc metal upon the axial coordination of pyridine and the resultant prevention of the electron transfer from pyrrole nitrogen to core zinc metal in ZnP.

In the complexation of ZnP-D1 with pyridine, similar trends are observed. Absorption maxima of ZnP-D1 in dichloromethane, upon addition of pyridine, were red-shifted from 420, 548, 590 nm to 428(+8), 560 (+12), 602 (+12) nm with the appearance of isosbestic points in 425 and 555 nm, and the intensity ratio  $\epsilon_\alpha/\epsilon_\beta$  increased 2.0 fold from 0.23 to 0.47 (see Figure 3(b) and Table 1). Fluorescence maxima of ZnP-D1 were also red-shifted from 598 and 648 nm to 608 (+10) and 651 (+3) nm on addition of pyridine at excitation wavelength of 410 nm (Figure 4(b) and Table 1). The fluorescence emission of ZnP-D1 was also red-shifted up to 10 nm. Fluorescence intensity of short wavelength band was slightly increased to *ca.* 1.1 fold with addition of pyridine.

Upon axial coordination of pyridine to ZnP-D4, the change of absorption and fluorescence spectra was shown in

Figure 3(c), Figure 4(c), and Table 1. As the concentration of pyridine increases, absorption maxima of ZnP-D4 in dichloromethane were red-shifted from 426, 552, 592 nm to 431 (+5), 564 (+12), 603 (+11) nm with the appearance of isosbestic points in 429 and 558 nm, and the intensity ratio  $\varepsilon_{\alpha}/\varepsilon_{\beta}$  increased 1.5 fold from 0.35 to 0.53. Fluorescence maxima of ZnP-D4 were also red-shifted from 602 and 650 nm to 611 (+9) and 661 (+11) nm and its intensity increased to *ca.* 1.2 fold, on addition of pyridine (Figure 4(c) and Table 1).

The complex formation constants  $K_f$  for axial coordination of pyridine on ZnP, ZnP-D1, and ZnP-D4 were estimated from the absorption spectral data by using Benesi-Hildebrand plot.<sup>39</sup>

$$1/(A_0 - A) = 1/(A_0 - A_{\infty}) + 1/(A_0 - A_{\infty}) \times 1/K_f \times 1/[py]$$

where, [py] is the concentration of pyridine,  $A_0$  is the absorbance of pure ZnP when [py]=0, A is the absorbance of the solution with arbitrary concentration of pyridine, and  $A_{\infty}$  is the absorbance of the practically pure coordinated complex between ZnP and pyridine when the concentration of pyridine is very high.

Using above equation, the complex formation constants  $K_f$  (Table 1) for axial coordination of pyridine on ZnP, ZnP-D1, and ZnP-D4 were estimated to be  $4.4 \times 10^3 \text{ M}^{-1}$ ,  $3.3 \times 10^3 \text{ M}^{-1}$ , and  $1.7 \times 10^3 \text{ M}^{-1}$ , respectively. The  $K_f$  values show the formation of fairly stable coordination complexes, even though  $K_f$  of ZnP-D4, where the core zinc porphyrin is surrounded by 4 aryl ether dendrons, is relatively small. As the number of aryl ether dendron surrounding the core zinc porphyrin increases, the complex formation constant  $K_f$  decreases because spatial crowdedness inhibits ligation of pyridine.

**Electron Transfer Between Zinc Porphyrin Dendrimer and Methyl Viologen.** Zinc porphyrins act as electron donor in the photoinduced electron transfer.<sup>7,40-44</sup> The photoinduced electron transfer of porphyrin dendrimer has been actively studied in a view of the diverse applications to artificial photosynthesis and optoelectronics.<sup>17-34</sup> Methyl viologen employed in this study is typical electron acceptor.<sup>45,46</sup>

Photoinduced electron transfer between ZnP, ZnP-D1, or ZnP-D4 and methyl viologen dichloride was described in Figure 5. Figure 6 shows the UV-vis absorption spectra of

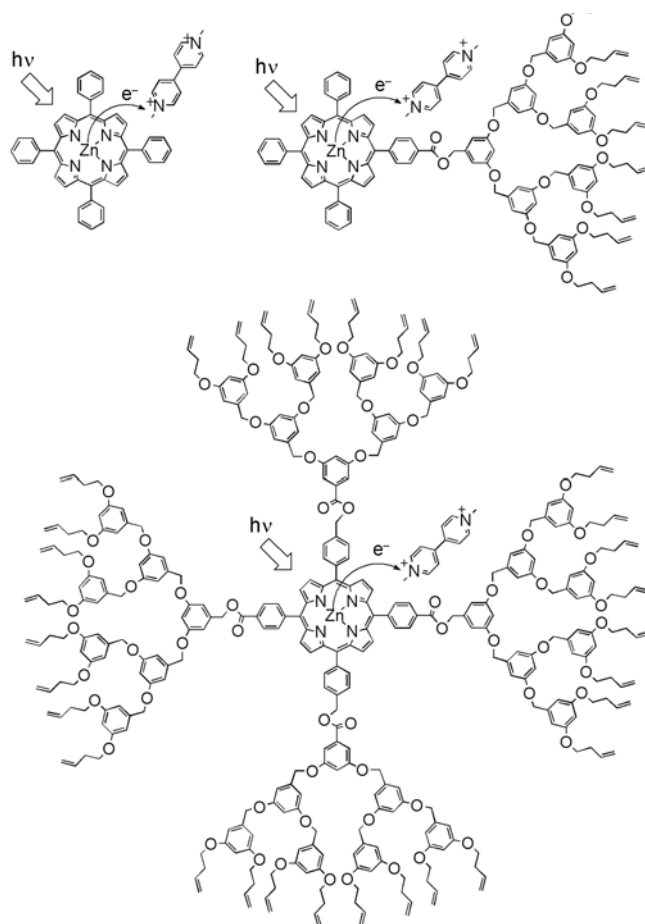


**Figure 5.** Photoinduced electron transfer between ZnP, ZnP-D1, or ZnP-D4 and methyl viologen.

ZnP, ZnP-D1, or ZnP-D4 of  $\sim 1 \times 10^{-5} \text{ M}$  in dichloromethane with addition of methyl viologen dichloride (0, 1, 2, 5, 10, 15, 20, 25, 30, 40, 50, 60, 70, 80, 90, 100 equiv.) in dichloromethane. Photoinduced electron transfer was investigated by observing the quenching of fluorescence spectra of ZnP, ZnP-D1, or ZnP-D4 by methyl viologen dichloride (0-100 equiv.) in Figure 7. Table 2 summarized absorption and fluorescence maxima for ZnP, ZnP-D1, ZnP-D4 before and after the addition of methyl viologen dichloride in dichloromethane, and Stern-Volmer constant  $K_{SV}$  for fluorescence

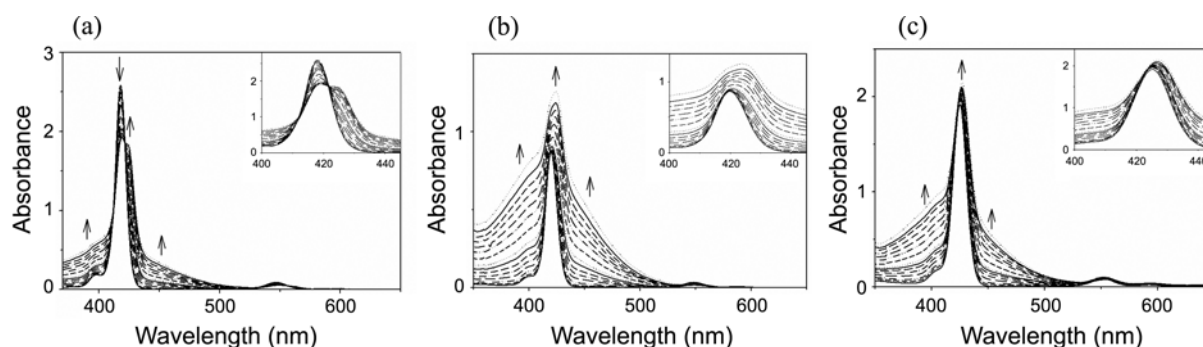


**Figure 6.** Absorption spectral change of ZnP (a), ZnP-D1 (b), and ZnP-D4 (c) of  $\sim 1 \times 10^{-5} \text{ M}$  with addition of methyl viologen dichloride (0, 1, 2, 5, 10, 15, 20, 25, 30, 40, 50, 60, 70, 80, 90, 100 equiv.) in dichloromethane.

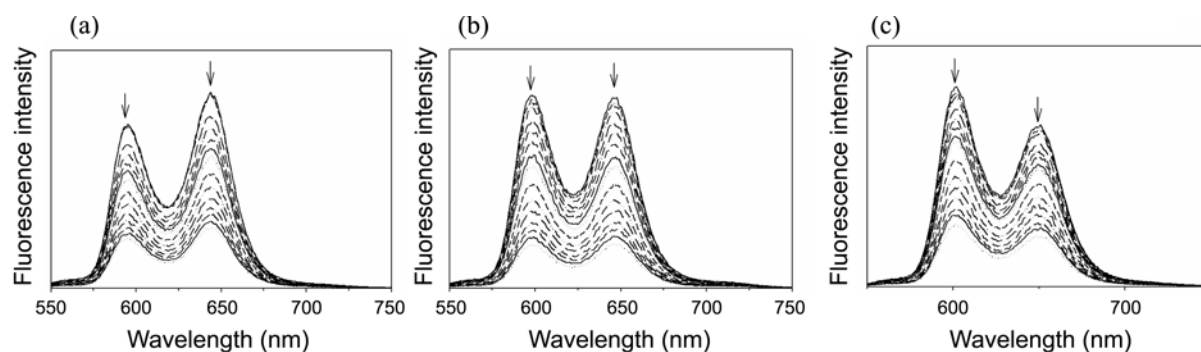


**Figure 7.** Fluorescence spectral change of ZnP (a), ZnP-D1 (b), or ZnP-D4 (c) of  $\sim 1 \times 10^{-5}$  M with addition of methyl viologen dichloride (0, 1, 2, 5, 10, 15, 20, 25, 30, 40, 50, 60, 70, 80, 90, 100 equiv.) in dichloromethane.

quenching.

As shown in Figure 6(a) and Table 2, upon addition of methyl viologen dichloride, Soret band and two Q bands of ZnP in dichloromethane were very slightly red-shifted from 418, 547, 585 nm to 424, 549, and 593 nm. Fluorescence of ZnP was quenched by addition of methyl viologen dichloride (Figure 7(a) and Table 2), provably due to the photoinduced electron transfer from electron donor ZnP to electron acceptor methyl viologen dichloride. From Stern-Volmer plot,  $K_{sv}$  for ZnP was calculated to be  $2.6 \times 10^3$ .

$$\frac{I_f^0}{I_f} = 1 + K_{sv}[Q]$$

where,  $[Q]$  is the concentration of methyl viologen dichloride,  $I_f^0$  is the fluorescence intensity of pure ZnP when  $[Q]=0$ ,  $I_f$  is fluorescence intensity of ZnP solution with arbitrary concentration of methyl viologen dichloride.

As shown in Figure 6(b) and Table 2, absorption maxima of ZnP-D1 in dichloromethane, upon addition of methyl viologen dichloride, were a little red-shifted from 420, 548, 590 nm to 424, 552, 596 nm. For fluorescence of ZnP-D1, the maxima were unchanged, but the intensity was quenched by addition of methyl viologen iodide, provably due to the photoinduced electron transfer, to give  $K_{sv}$  of  $2.5 \times 10^3$  (Figure 7(b) and Table 2).

With addition of methyl viologen dichloride, the change of

absorption and fluorescence spectra of ZnP-D4 was shown in Figure 6(c), Figure 7(c), and Table 2. As the concentration of methyl viologen dichloride increases, absorption maxima of ZnP-D4 in dichloromethane were nearly unchanged from 426, 552, 592 nm to 427, 554, 596 nm. Fluorescence maxima of ZnP-D4 were also unchanged and  $K_{sv}$  for fluorescence quenching was estimated to be  $2.1 \times 10^3$ .

To compare the efficiency of photoinduced electron transfer between ZnP, ZnP-D1, or ZnP-D4 and methyl viologen dichloride,  $K_{sv}$  was obtained from Stern-Volmer plots for fluorescence quenching.  $K_{sv}$  was estimated to be  $2.6 \times 10^3$ ,  $2.5 \times 10^3$ , and  $2.1 \times 10^3$ , for ZnP, ZnP-D1, and ZnP-D4, respectively. From these values of Stern-Volmer constants  $K_{sv}$ , it was assumed that the efficiency of photoinduced electron transfer between ZnP and methyl viologen dichloride was similar to that between ZnP-D1 and methyl viologen iodide. In the case of ZnP-D4 containing 4 aryl ether dendrons surrounding the core zinc porphyrin, judging from smaller Stern-Volmer constants  $K_{sv}$ , photoinduced electron transfer to methyl viologen dichloride might be less efficient than ZnP and ZnP-D1 because of spatial crowdedness. Nonetheless, all three ZnP, ZnP-D1, and ZnP-D4 show efficient photoinduced electron transfer to methyl viologen dichloride to some extent.

Further studies with zinc porphyrin-cored aryether dendrimers, such as construction of higher order dendrimers through noncovalent coordination of pyridine-tethered dendrons and noncovalent interaction with other electron acceptors, are under investigation.

## Conclusions

The porphyrin-incorporated aryether dendrimers ZnP-D1 and ZnP-D4, the compounds containing zinc porphyrin in the core and benzyl aryether dendrons with 3,5-bis(but-3-enyloxy)phenyl groups in the periphery, were investigated the influence of dendritic environments for the axial ligation of pyridine and photoinduced electron transfer by methyl viologen.

Absorption and fluorescence spectra of ZnP, ZnP-D1, and ZnP-D4 were measured in dichloromethane with the addition of pyridine or methyl viologen dichloride. Axial ligation

**Table 2.** Absorption maxima ( $\lambda_a^{\max}$ ) and fluorescence maxima ( $\lambda_f^{\max}$ ) for ZnP, ZnP-D1, and ZnP-D4 before and after the addition of methyl viologen dichloride in dichloromethane, and Stern-Volmer constants ( $K_{sv}$ ) for fluorescence quenching

Compound	[methyl viologen dichloride]/[compound]	$\lambda_a^{\max}$ , nm			$\lambda_f^{\max}$ , nm	$K_{sv}$ , $M^{-1}$
		Soret band	Q band			
			$\beta$	$\alpha$		
ZnP	0	418	547	585	596, 644	$2.6 \times 10^3$
	100	424	549	593	596, 645	
ZnP-D1	0	420	548	590	598, 648	$2.5 \times 10^3$
	100	424	552	596	598, 649	
ZnP-D4	0	426	552	592	602, 650	$2.1 \times 10^3$
	100	427	554	596	602, 649	

of pyridine was confirmed by red-shifted absorption spectrum and photoinduced electron transfer to methyl viologen dichloride by fluorescence quenching.

ZnP-D4 surrounding by 4 aryl ether dendrons shows smallest  $K_f$  and  $K_{sv}$ , with comparison to ZnP and ZnP-D1. Dendritic environments should inhibit both complexation and photoinduced electron transfer of zinc porphyrin to some extent. Nevertheless, even ZnP-D4 successfully conduct axial ligation of pyridine and photoinduced electron transfer to methyl viologen dichloride, so that porphyrin dendrimer ZnP-D4 is unsparing as model compound of natural hemoproteins or natural photosynthetic systems.

**Acknowledgments.** This work is financially supported by the Ministry of Education, Science and Technology (MEST), the Ministry Knowledge Economy (MKE) through the fostering project of the Industrial-Academic Cooperation Centered University.

### References

- Wasielowski, M. *J. Org. Chem.* **2006**, *71*, 5051.
- Lomoth, R.; Magnuson, A.; Sjoedin, M.; Huang, P.; Styring, S.; Hammarstrom, L. *Photosynth. Res.* **2006**, *87*, 25.
- Alstrum-Acevedo, J. H.; Brennaman, M. K.; Meyer, T. J. *Inorg. Chem.* **2005**, *44*, 6802.
- Choi, M.-S.; Yamazaki, T.; Yamazaki, I.; Aida, T. *Angew. Chem., Int. Ed.* **2003**, *43*, 150.
- Imahori, H.; Mori, Y.; Matano, Y. *J. Photochem. Photobiol., C* **2003**, *4*, 51.
- Willner, I.; Willner, B. *Top. Curr. Chem.* **1991**, *159*, 153.
- Balzani, V.; Scandola, F.; Fox, M. A.; Chanon, M., Eds., In *Photoinduced Electron Transfer Part A-D*, Elsevier: Amsterdam, 1988; pp 148-178.
- D'Souza, F.; Smith, P. M.; Zandler, M. E.; McCarty, A. L.; Itou, M.; Araki, Y.; Ito, O. *J. Am. Chem. Soc.* **2004**, *126*, 7898.
- Gust, D.; Moore, T. A.; Moore, A. L. *Acc. Chem. Res.* **1993**, *26*, 198 and **2001**, *34*, 40.
- Pleux, L. L.; Pellegrin, Y.; Blart, E.; Odobel, F.; Harriman, A. *J. Phys. Chem. A* **2001**, *115*, 5069.
- Imahori, H. *Org. Biomol. Chem.* **2004**, *2*, 1425.
- Guldi, D. M. *Chem. Soc. Rev.* **2002**, *31*, 22.
- Newkome, G. R.; Moorefield, C. N.; Vögtle, F. *Dendrimers and Dendrons-Concepts, Synthesis, Applications*; Wiley-VCH: Weinheim, 2001.
- Astruc, D.; Boisselier, E.; Ornelas, C. *Chem. Rev.* **2010**, *110*, 1857.
- Balzani, V.; Ceroni, P.; Juris, A.; Venturi, M.; Campagna, S.; Puntoriero, F.; Serroni, S. *Coord. Chem. Rev.* **2001**, *219-221*, 545.
- Maes, W.; Dehaen, W. *Eur. J. Org. Chem.* **2009**, 4719.
- Nagata, T.; Kikuzawa, Y. *Biochim. Biophys. Acta* **2007**, *1767*, 648.
- Kozaki, M.; Akita, K.; Suzuki, S.; Okada, K. *Org. Lett.* **2007**, *9*, 3315.
- Larsen, J.; Brueggemann, B.; Sly, J.; Crossley, M. J.; Sundstroem, V.; Aakesson, E. *Chem. Phys. Lett.* **2006**, *433*, 159.
- Campidelli, S.; Sooambar, C.; Diz, E. L.; Ehli, C.; Guldi, D. M.; Prato, M. *J. Am. Chem. Soc.* **2006**, *128*, 12544.
- Li, W.-S.; Kim, K. S.; Jiang, D.-L.; Tanaka, H.; Kawai, T.; Kwon, J. H.; Kim, D.; Aida, T. *J. Am. Chem. Soc.* **2006**, *128*, 10527.
- Cho, S.; Li, W.-S.; Yoon, M.-C.; Ahn, T. K.; Jiang, D.-L.; Kim, J.; Aida, T.; Kim, D. *Chem.-Eur. J.* **2006**, *12*, 7576.
- Oar, M. A.; Dichtel, W. R.; Serin, J. M.; Fréchet, J. M. J.; Rogers, J. E.; Slagle, J. E.; Fleitz, P. A.; Tan, L.-S.; Ohulchanskyy, T. Y.; Prasad, P. N. *Chem. Mater.* **2006**, *18*, 3682.
- Ogasawara, S.; Ikeda, A.; Kikuchi, J.-I. *Chem. Mater.* **2006**, *18*, 5982.
- Figueira-Duarte, T. M.; Clifford, J.; Amendola, V.; Gégout, A.; Olivier, J.; Cardinali, F.; Meneghetti, M.; Armaroli, N.; Nierengarten, J.-F. *Chem. Commun.* **2006**, 2054.
- Flamigni, L.; Talarico, A. M.; Ventura, B.; Sooambar, C.; Solladie, N. *Eur. J. Inorg. Chem.* **2006**, 2155.
- Mo, Y.-J.; Jiang, D.-L.; Uyemura, M.; Aida, T.; Kitagawa, T. *J. Am. Chem. Soc.* **2005**, *127*, 10020.
- Hasobe, T.; Kamat, P. V.; Absalom, M. A.; Kashiwagi, Y.; Sly, J.; Crossley, M. J.; Hosomizu, K.; Imahori, H.; Fukuzumi, S. *J. Phys. Chem. B* **2004**, *108*, 12865.
- Capitost, G. J.; Cramer, S. J.; Rajesh, C. S.; Modarelli, D. A. *Org. Lett.* **2001**, *3*, 1645.
- Sadamoto, R.; Tomioka, N.; Aida, T. *J. Am. Chem. Soc.* **1996**, *118*, 3978.
- Tsuda, A.; Alam, M. A.; Harada, T.; Yamaguchi, T.; Ishii, N. *Angew. Chem. Int. Ed.* **2007**, *46*, 8198.
- Lee, D.-I.; Goodson, T. III. *J. Phys. Chem. B* **2006**, *110*, 25582.
- Li, Y.; Rizzo, A.; Salerno, M.; Mazzeo, M.; Huo, C.; Wang, Y.; Li, K.; Cingolani, R.; Gigli, G. *Appl. Phys. Lett.* **2006**, *89*, 1.
- Oh, J. B.; Kim, Y. H.; Nah, M. K.; Kim, H. K. *J. Luminescence* **2005**, *111*, 255.
- Lim, S.; Choi, D.; Shin, E. J. *Bull. Korean Chem. Soc.* **2008**, *29*, 1353.
- Nappa, M.; Valentine, J. S. *J. Am. Chem. Soc.* **1978**, *100*, 5075.
- D'Souza, F.; Hsieh, Y.-Y.; Deviprasad, G. R. *Inorg. Chem.* **1996**, *35*, 5747.
- Ambrose, A.; Li, J.; Yu, L.; Lindsey, J. S. *Org. Lett.* **2000**, *2*, 2563.
- Benesi, H. A.; Hildebrand, J. H. *J. Am. Chem. Soc.* **1949**, *71*, 2703.
- Wasielowski, M. *Chem. Rev.* **1992**, *92*, 435.
- Rajesh, C. S.; Capitost, G. J.; Cramer, S. J.; Modarelli, D. A. *J. Phys. Chem. B* **2001**, *105*, 10175.
- Sessler, J. L.; Johnson, M. R.; Lin, T. Y.; Creager, S. E. *J. Am. Chem. Soc.* **1988**, *110*, 3659.
- Straight, S. D.; Andréasson, J.; Kodis, G.; Moore, A. L.; Moore, T. A.; Gust, D. *J. Am. Chem. Soc.* **2005**, *127*, 2717.
- Pasunooti, K. K.; Song, J.-L.; Chai, H.; Amaladass, P.; Deng, W.-Q.; Liu, X.-W. *J. Photochem. Photobiol. A: Chem.* **2011**, *218*, 219.
- Kaganer, E.; Joselevich, E.; Willner, I.; Chen, Z.; Gunter, M. J.; Gayness, T. P.; Johnson, M. R. *J. Phys. Chem. B* **1998**, *102*, 1159.
- Hosono, H.; Kaneko, M. *J. Photochem. Photobiol. A: Chem.* **1997**, *107*, 63.